Phase Identification in a Series of Liquid Crystalline TPP Polyethers and Copolyethers Having Highly Ordered Mesophase Structures. 8. Phase and Structural Evolution in a Series of Copolyethers Containing Odd-Numbered Methylene Units in Both Comonomers

Ru-Qing Zheng,[†] Er-Qiang Chen,[†] Stephen Z. D. Cheng,*[,†] Fengchao Xie,[‡] Donghang Yan,[‡] Tianbai He,[‡] Virgil Percec,[§] Peihwei Chu,[§] and Goran Ungar[⊥]

Maurice Morton Institute and Department of Polymer Science, The University of Akron, Akron, Ohio 44325-3909; National Key Laboratory of Polymer Physics and Chemistry, Chinese Academy of Sciences, Changchun, Jilin, 130022, P. R. China; Department of Chemistry, University of Pennsylvania, Philadelphia, Pennsylvania 19104-6323; and Department of Engineering Materials, University of Sheffield, Sheffield S1 3JD, UK

Received November 23, 1999; Revised Manuscript Received May 12, 2000

ABSTRACT: A series of liquid crystalline copolyethers have been synthesized from 1-(4-hydroxy-4′-biphenyl)-2-(4-hydroxyphenyl)propane with 1,7-dibromoheptane and 1,11-dibromoundecane (coTPPs-7/11). This represents the copolyethers containing only odd numbers of methylene units in both comonomers. The molar ratio between these two comonomers in this series ranges from 1/9 to 9/1. The coTPPs-7/11 exhibit multiple phase transitions during cooling and heating in differential scanning calorimetry experiments. In each of these thermal transitions, only a small undercooling and superheating dependence is observed upon cooling and heating at different rates. All of the coTPPs-7/11 possess similar phase behavior based on the structural analyses using wide-angle X-ray diffraction (WAXD) on both powder and fiber samples and electron diffraction experiments on thin-film samples in transmission electron microscopy. The low-temperature phase is identified as a tilted hexagonal columnar (Φ_{TH}) phase with multiple tilt angles between molecular axes and the hexagonal lattice normal. However, the hexagonal lateral dimensions in a Φ_{TH} phase with various tilt angles are identical. This Φ_{TH} phase transforms to another columnar (Φ') phase during heating at approximately 140 °C, as evidenced by the temperature-resolved WAXD fiber patterns. In this transition, the laterally ordered reflections from the (110) and (200) planes in the quadrants move toward the equator, corresponding to the decreased tilt angles. The discontinuous change in both the lateral *d* spacings and tilt angles represents a first-order transition. The columnar−columnar phase transition may be associated with the conformational disorder of the methylene units according to the infrared spectroscopic observations. Further heating of the samples leads to transitions from the Φ' to a nematic (N) phase and from the N phase to the isotropic melt. Combining the copolymer phase behaviors observed with the corresponding homopolymers TPPs($n = 7$ and 11), a phase diagram describing transition temperatures with respect to the composition can be constructed. Their transition properties are also discussed.

Introduction

In the previous publications, we have reported the phase identifications of a series of main-chain liquid crystalline (LC) polyethers synthesized from 1-(4-hydroxy-4′-biphenyl)-2-(4-hydroxyphenyl)propane (i.e., TPP mesogen) and α,ω-dibromoalkanes [TPP(*n*)], where highly ordered smectic F (S_F), smectic crystal G (SC_G), and H (SC_H) phases have been assigned.[1−3] The phase structure and transition behavior are strongly dependent on the number of methylene units. We summarize the most important experimental results from the TPPs($n = 7$ and 11) since the current study involves copolyethers synthesized from the TPP mesogen with 1,7-dibromoheptane and 1,11-dibromoundecane (coTPPs-7/11). The TPP($n = 7$) exhibits the following phase transition sequence:[2]

$$\text{glassy state} \leftrightarrow SC_G \leftrightarrow S_F \leftrightarrow N \leftrightarrow I$$

and a SC_H phase is added for the TPP($n = 11$) at low temperatures:[2]

$$\text{glassy state} \leftrightarrow SC_H \leftrightarrow SC_G \leftrightarrow S_F \leftrightarrow N \leftrightarrow I$$

The chain orientation in the S_F and SC_G phases of TPP($n = 7$) is tilted approximately 14° and 16° from the fiber direction, respectively.[2] The tilt angle becomes 7° for TPP($n = 11$) in the S_F phase, but the molecular axis is parallel to the fiber direction in the SC_G and SC_H phases.[2] The transition thermodynamic properties (temperatures and heats of transitions),[2−6] molecular dynamics in different phases,[7] surface-induced phase structures,[8] and structural and morphological evolutions in TPPs[9] have also been investigated.

The first columnar (Φ) LC phases were identified in small molecular disklike compounds in 1977.[10] Liquid crystals and LC polymers containing discotic mesogens have since become a topic of considerable interest.[11−18] However, recent studies have revealed that many conventional flexible polymers also exhibit Φ phases, which do not require the presence of discotic meso-

[†] The University of Akron.
[‡] Chinese Academy of Sciences.
[§] University of Pennsylvania.
[⊥] University of Sheffield.
* To whom correspondence should be addressed. E-mail cheng@polymer.uakron.edu.

10.1021/ma991963p CCC: $19.00
Published on Web 06/23/2000

gens.[19,20] The Φ phases are characterized by the existence of lateral long-range order in two dimensions and an absence of such order in the third direction. From a symmetry point of view, the calamitic Φ phases with rodlike mesogens are identical to those known to form by small molecular discotic liquid crystals. TPP copolymers with various methylene unit lengths is one example of main-chain LC polymers containing rodlike mesogens to exhibit hexagonal columnar phases (Φ_H).[21,22] These copolymers generate aperiodicity and disturb the long-range order along the chain direction compared to their homopolymer counterparts. The Φ_H phases result from the cylindrical columns formed by individual chain stems, in contrast to discotic Φ phases where the columns are formed by the stacking of disklike molecules.

In our recent work on the coTPPs-*n*/12(5/5) (copolyethers containing a varying odd number ($n = 5$, 7, 9, and 11) and a fixed even number ($m = 12$) of methylene units with fixed compositions at an equal molar ratio of 5/5),[21] highly ordered smectic phases are found when the comonomer lengths are close, such as in the coTPP-11/12(5/5). However, a Φ_H phase is observed for the increased dissimilarity of comonomer lengths, because the mismatch of the mesogenic groups destroys the longitudinal order along the chain direction, as in the coTPP-5/12(5/5) and coTPP-7/12(5/5). We have also reported a series of coTPPs-7/12 with different comonomer compositions,[22] where highly order smectic, Φ_H, and tilted hexagonal columnar (Φ_{TH}) phases were found to be composition-dependent. The chain orientation is tilted with respect to the hexagonal normal in a tilted phase.

In this study, the coTPPs-7/11 with only odd numbers of methylene units are investigated. By changing the composition of two comonomers, we monitor the phase structural evolution and transition behavior. Furthermore, the difference between the odd−odd and odd−even (e.g., coTPPs-7/12) systems can be recognized through this study. The goal is to increase our understanding in identifications and classification of new phases and phase transformations related to columnar phases.

Experimental Section

Materials. The series of coTPP-7/11 were synthesized by random copolymerization from 1-(4-hydroxy-4′-biphenyl)-2-(4-hydroxyphenyl)propane with 1,7-dibromoheptane and 1,11-dibromoundecane. The detailed synthetic procedure of TPP mesogens and homoTPPs has been published elsewhere.[23] The chemical structure of the coTPPs-7/11 is

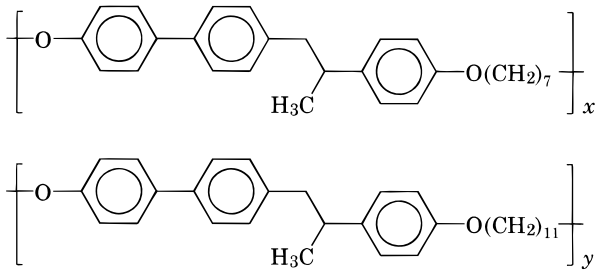

The compositions (*x*/*y*) of coTPPs-7/11 varied from 1/9 to 9/1 in the molar ratio. Samples studied were characterized via gel permeation chromatography in chloroform based on polystyrene standards. Their number-average molecular weights (M_n) ranged between 20 000 and 30 000 g/mol.

Instrument and Experiments. Thermal behaviors were examined by using a differential scanning calorimetry (DSC). Experiments were performed on a Perkin-Elmer DSC-7 instrument. The temperature and heat flow were calibrated using standard materials at different scan rates. Initial sample weights of approximately 3 mg were used. The cooling and heating experiments were conducted at various rates between 2.5 and 40 °C/min in a nitrogen atmosphere. The transition temperatures were determined by measuring the onset cooling temperatures and extrapolating them to 0 °C/min.

Wide-angle X-ray diffraction (WAXD) experiments were carried out using a 12 kW rotating-anode generator (Cu Kα) in combination with a Geigerflex D/max-RB diffractomter. The reflection peak positions and widths were calibrated with silicon powder ($2\theta > 15°$) and silver behenate ($2\theta < 10°$). WAXD powder samples were prepared by heating and then pressing the samples at nematic (N) temperatures. Powder patterns were taken at a scan rate of 10°/min within the 2θ angle region of 2°−30°. Heating and cooling experiments were conducted at a rate of 2.5 °C/min utilizing a hot stage in conjunction with the diffractometer. Background scattering was recorded and subtracted from the sample patterns.

Fiber WAXD patterns were obtained using an imaging plate (Rigaku automated imaging system with 3000 × 3000 pixel resolution) equipped with a built-in hot stage. Calibration again was conducted using silicon powder and silver behenate. Fibers were prepared by drawing the samples from the LC phase where applicable. Samples were then heated to elevated temperatures and illuminated with a point-focusing X-ray beam. A typical exposure time for fiber samples was 30 min.

An Olympus BH-2 polarized light microscopy (PLM) with a Mettler hot stage (FP-90) was used to observe and analyze morphological changes during thermal transitions. The films were prepared using melt-pressed coTPPs between two glass slides. Several mechanically sheared samples were also examined to identify the N phase. Sheared samples were prepared by heating samples at temperatures characteristic of the N phases then shearing them with a razor.

Transmission electron microscopy (TEM) was performed with a JEOL (1200 EX II) instrument at an accelerating voltage of 120 kV. CoTPP thin films were solution cast on amorphous carbon-coated surfaces at a concentration of 0.1% (w/w) in tetrahydrofuran. The thin films were shadowed with Pt and coated with carbon for TEM observations. Spacing was calibrated using TlCl for electron diffraction (ED) experiments.

A Mattoson Galaxy 5000 instrument coupled with a hot stage was employed for Fourier transform infrared (FTIR) spectroscopy measurements. The films of coTPPs were solution cast on sodium chloride (NaCl) pellets followed by drying under vacuum. The samples were heated to the isotropic melt and then cooled to room temperature before heating to preset temperatures for IR study. Spectra were recorded with a resolution of 2 cm^{-1} and 40 scans at each sampled temperature.

Results and Discussion

Thermal Transitions in coTPPs(7/11). As one example, Figure 1 shows a set of DSC cooling and subsequent heating thermal diagrams of the coTPP-7/11(1/9) at different rates. Each of these thermal diagrams apparently exhibits two major exothermic (in cooling) or endothermic (in heating) events. However, the high-temperature transition at approximately 170 °C actually consists of two overlapped transitions, which can be identified on slow cooling such as at 2.5 °C/min. The onset temperatures of transitions in the coTPPs-7/11 show small undercooling (superheating) dependence at various cooling (heating) rates. For instance, the highest-temperature transition of coTPP-7/11(1/9) occurs at 168 °C (extrapolated to 0 °C/min), and it shows only a 2 °C undercooling dependence between 2.5 and 40 °C/min. In general, undercoolings of the onset tem-

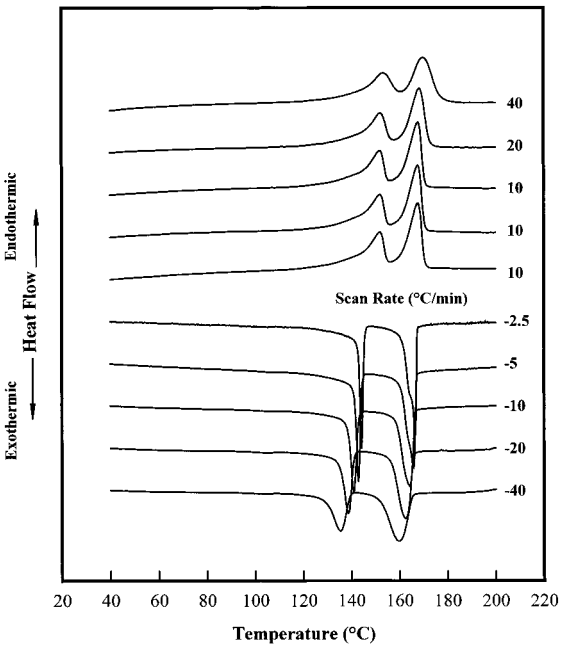

Figure 1. Set of DSC curves of the coTPP-7/11(1/9) at different cooling and heating rates.

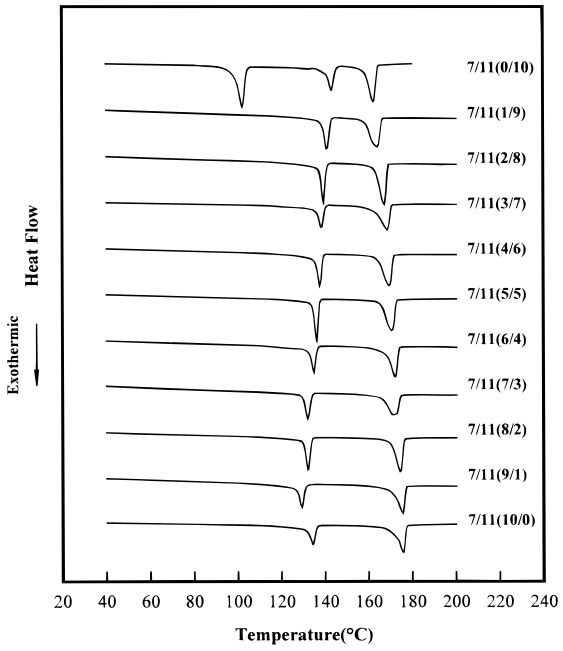

Figure 2. Set of DSC cooling curves for all of the coTPPs-7/11 and homoTPPs(n = 7 and 11) at 10 °C/min.

peratures for the coTPPs-7/11 are only a few degrees for the scans between 2.5 and 40 °C/min. These transitions are thus close to thermodynamic equilibrium and may be associated with the LC structural changes as in other main-chain LC polymers.[24−28]

To provide an overview of thermal behavior of coTPPs-7/11, Figure 2 shows DSC cooling diagrams of all the copolymers studied at 10 °C/min. Both diagrams of the homoTPPs(n = 7 and 11) are also included for comparison. It is evident that the lowest-temperature transition at approximately 100 °C for TPP(n = 11) does not exist in the coTPPs-7/11, implying the possible suppression of highly ordered LC phases in the copolymers. The high-temperature transition in every copolymer is attributed to the two overlapped transitions

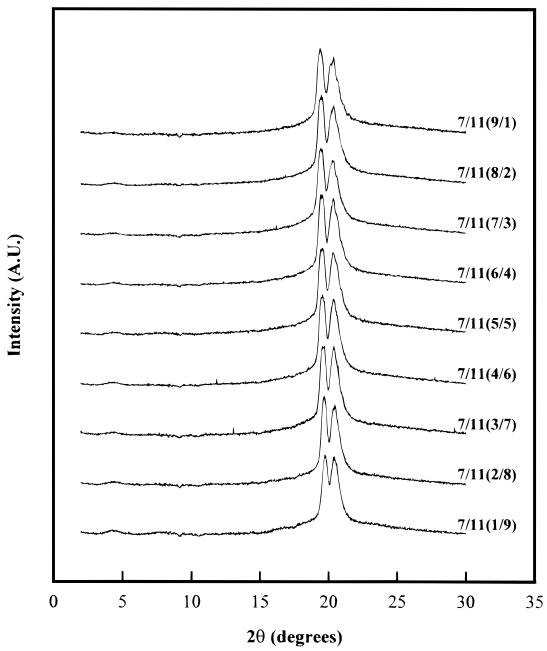

Figure 3. WAXD powder patterns of the coTPPs-7/11 taken at room temperature after the samples were cooled from the isotropic melt at 2.5 °C/ min.

having very close transition temperatures, as in the case of coTPP-7/11(1/9) (Figure 1). Therefore, with the low-temperature transition at approximately 140 °C, three transition processes can be determined in the coTPPs-7/11 on the basis of the DSC observations.

Low-Temperature Structure Identifications. Figure 3 describes a set of WAXD powder patterns obtained at room temperature after coTPP-7/11 samples were cooled from the isotropic melt. All of the WAXD patterns are similar, possessing two intense reflection peaks at 2θ angles of 19°−21°. These reflections have relatively broad full widths at half-height compared to those observed in the coTPPs-n/12.[21] The first reflection gradually changes its peak position from 19.7° in coTPP-7/11(1/9) to 19.4° in coTPP-7/11(9/1), whereas the second reflection shows much less change at approximately 20.4° as a function of composition. Since reflections in the high-angle region are usually associated with the neighboring lateral molecular packing, a decrease in the 2θ value of the first reflection should be associated with an increased lateral d-spacing, corresponding to a looser packing due to the increased incorporation of seven-numbered methylene units (shorter comonomer). WAXD fiber patterns are required to exactly identify the phase structure and type of order in these samples, since powder patterns do not provide the structural dimensionality of these ordered phases.

All of the coTPPs-7/11 exhibit similar WAXD fiber patterns at room temperature, as represented by the coTPPs-7/11(5/5 and 9/1) in parts a and b of Figure 4. Compared with those homoTPPs that exhibit highly ordered smectic and smectic crystalline phases, the two most striking features in the copolymer fiber patterns are the disappearance of the sharp low-angle layer reflections and the appearance of multiple wide-angle reflections in the quadrants. This illustrates the completely different phase structures of these coTPPs-7/11 from those of the homoTPPs(n = 7 and 11).[2] As shown in Figure 4, the multiple wide-angle reflections of the coTPPs-7/11 are almost aligned on a pair of "lines"

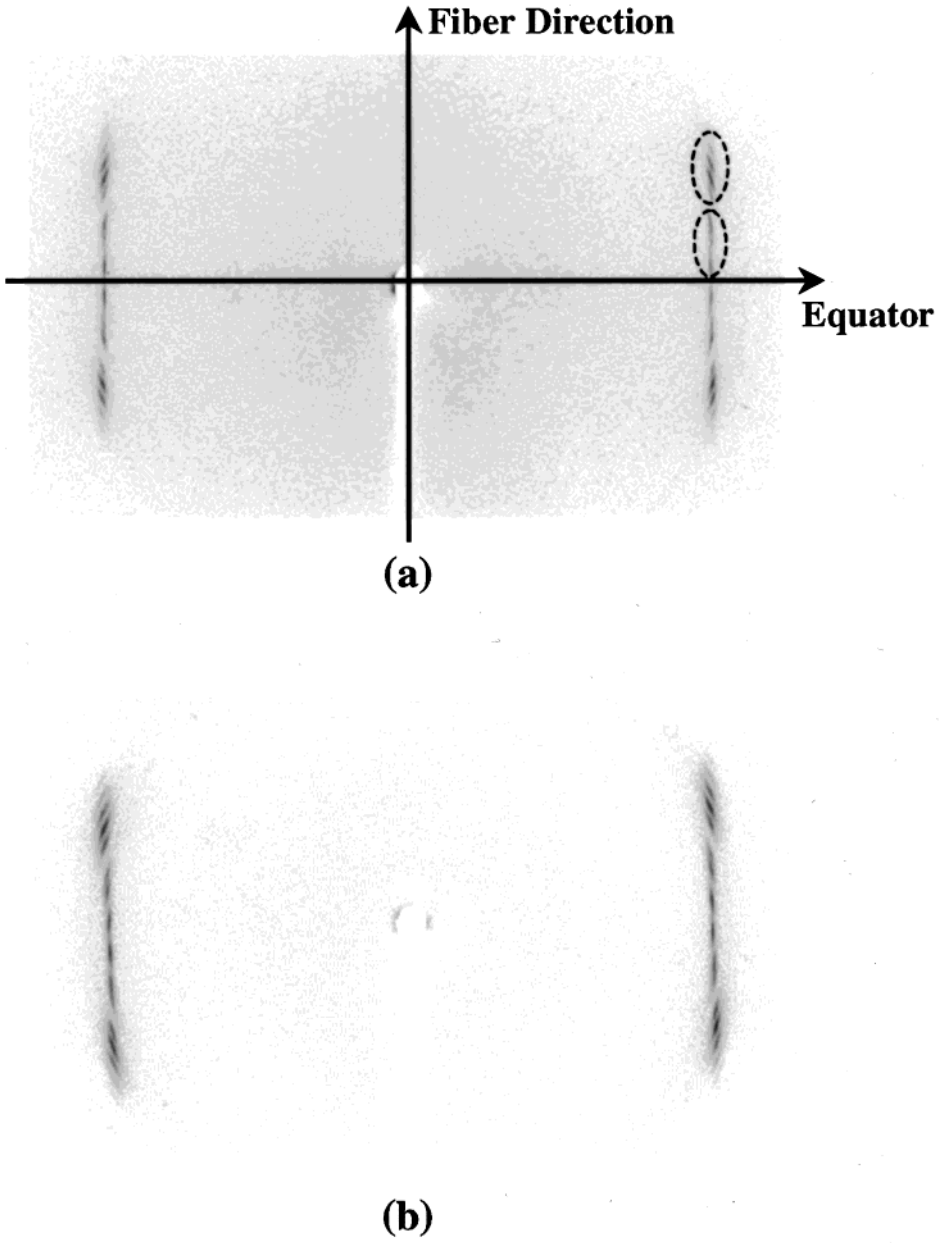

Figure 4. Room-temperature WAXD fiber patterns of (a) coTPP-7/11(5/5) and (b) coTPP-7/11(9/1).

nearly parallel to the meridian direction. In fact, these reflections in the quadrants construct the two relatively broad reflection peaks observed in the powder patterns in Figure 3 (see circles in Figure 4). The overlaps occur due to the very close 2θ values of the reflections and the limited resolution of WAXD powder patterns. This phenomenon has not been found in the coTPPs-*n*/12, each of which only presents a single narrow reflection on the equator.[21]

On the basis of the structural analysis and LC classification,[29−32] we propose that the coTPP-7/11 fiber patterns at room temperature be attributed to a two-dimensionally ordered Φ_{TH} phase possessing various tilt angles. The multiple reflections in any coTPP-7/11 sample can be separated into five or more sets, and each includes the (200) and (110) reflections. The off-equator and split of the (110) and (200) reflections are caused by the tilted molecular axes with respect to the meridian (also normal of the hexagonal lattice) as observed in several homoTPPs and coTPPs.[1−3,21,22] To elaborate, parts a and b of Figure 5 show the (110) and (200) planes in real space, and Figure 5c shows the corresponding reflections in reciprocal lattice. If σ and δ represent the angles for the (110) normal and chain direction with respect to the meridian, respectively, then $(90°-\sigma)$ and δ become the angles of the (110) and (200) reflections tilted away from the equator. The ratio of the (110) to (200) *d* spacings, the tilt angle of molecular axis (i.e., $\beta' = 90° + \delta$, where β' is the angle between the chain orientation and *a* axis), and the values of σ and δ possess a fixed geometric relationship. Therefore, the lateral lattice dimensions can be calculated. For instance, relationships of $\mathrm{tg}\sigma \cdot \mathrm{tg}\delta = 2$ and $d_{200}/d_{110} = 0.5(3\sin^2\beta' + 1)^{1/2}$ hold for a hexagonal lateral packing. Our analyses suggest that at room temperature the coTPPs-7/11 possess a two-dimensional hexagonal packing along the cross section perpendicular to the meridian. However, each set of the (200) and (110) reflections corresponds to the certain molecular axis tilted at a specific angle from the hexagonal lattice normal. Since the molecular axis is identical to the preferred orientation of mesogenic groups, the arrangement in which the

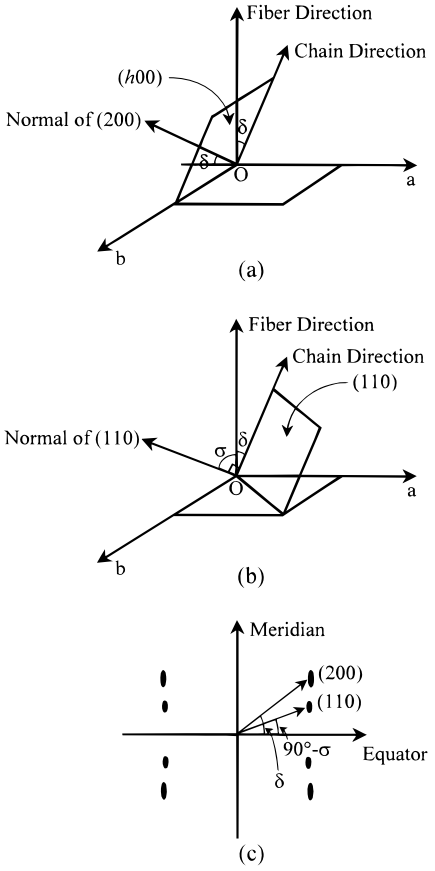

Figure 5. Structure and diffraction of a Φ_{TH} phase: (a) and (b) the (100) and (200) planes in real space and (c) the corresponding reflections in reciprocal space.

chains orient, tilt, and pack leads to the identification of a Φ_{TH} phase.

Table 1 lists the dimensional parameters of the coTPP-7/11(9/1) as an example, in which β' also represents the angle between the *a*-axis and the column direction. The *d* spacing ratios between the (110) and (200) reflections calculated assuming a hexagonal lattice are included in this table, which are consistent with the WAXD measurements. Surprisingly, the hexagonal lattice dimensions for the multiple sets of reflections in each sample are identical. In the coTPP-7/11(9/1), the dimensions of $a = 0.93$ nm and $b = 0.54$ nm are found.

ED experiments in TEM also support the assignment of the hexagonal lateral packing in these coTPPs-7/11. Figure 6 describes the TEM observations and ED patterns of coTPP-7/11(5/5). The single domain (Figure 6a) and polydomain textures (Figure 6b) are the two common morphologies of the sample, with the latter often containing the lamellae with different orientations. Two kinds of ED patterns are correspondingly observed. One is the hexagonal lattice (Figure 6c), with a measured *d* spacing in agreement with WAXD experiments. This indicates that the ED pattern obtained from Figure 6a possesses a [00*l*] zone, and the molecular axes are more or less perpendicular to the substrate surface (homeotropic orientation). The other type of ED pattern obtained from Figure 6b exhibits multiple diffraction spots (Figure 6d) and is similar to the WAXD fiber patterns although no external force field is applied. In this case, the molecular axes of the copolymer are oriented parallel to the substrate surface (homogeneous orientation).

The copolymerization from two comonomers with different numbers of methylene units interrupts the ordered packing of mesogenic groups and results in the absence of the ordered layer structures in this series of coTPPs-7/11. We propose that the chains are at least locally extended along their contour length and are close to cylindrical in shape since the copolymerization introduces aperiodicity along the chain direction. These cylindrical-shaped molecules pack parallel to one another to form the Φ_{TH} phase, where the column direction is parallel to the molecular axis. Molecules possess the identical orientation within each individual domain but may bend or even partially fold due to the conformational defects and thus change the molecular orientation. This may lead to domains with various orientations corresponding to the multiple tilt angles. Further investigation is necessary to better understand the molecular packing. Nevertheless, the randomness is obvious in these copolymers since no highly ordered smectic crystalline phases can be observed as in the cases of the homoTPPs($n = 7$ and 11).

Structural Evolution during Phase Transitions. The WAXD nonisothermal experiments were carried out to study the structural changes during each phase transition. The WAXD patterns recorded during heating and cooling are virtually identical, indicating that these transitions are thermodynamically reversible. Only the heating powder patterns are discussed here, together with the fiber patterns upon heating. Because of the similar phase behavior in this series, the coTPP-7/11(7/3) is chosen to be a representative. Figure 7 shows a set of WAXD powder patterns during heating. According to the room-temperature structural analysis, the two relatively broad reflection peaks in the wide-angle region represent the multiple reflections in the quadrants of the fiber pattern. The first peak includes the (110) and (200) reflection set with the smallest tilt angle ($\beta' = 94°$) and several (110) reflections with other tilt angles, whereas the second peak includes the rest of the (200) reflections. Upon heating, the peak positions of these two powder reflections shift slightly to the lower 2θ angles, corresponding to an increase in *d* spacings. However, the shift rates of the two peaks are different, and they gradually approach each other with increasing temperature. The ordered structure melts and only amorphous halo remains prior to a complete merge of these two reflection peaks.

The enlarged WAXD fiber patterns of coTPP-7/11(7/3) shown in Figure 8 describe the low-temperature phase transition, which can be observed at approximately 130 °C in the DSC diagram at a cooling rate of 10 °C/min (see Figure 2). However, both the exothermic peaks upon cooling and the endothermic peaks upon heating of the coTPPs-7/11 possess a broadening "tail" on the lower temperature side in the DSC experiments (see Figure 1 as an example), which results in the earlier occurrence of the transition upon heating. Apparently, from 100 to 130 °C, the set of the (110) and (200) reflections nearest to the equator with $\beta' = 94°$ (see arrows in Figure 8a) moves toward the equator (i.e., decreases the tilt angle) and finally merges into the equator (see the arrow in Figure 8d). Meanwhile, other reflections are also found to correspondingly decrease with their tilt angles in this temperature region. For example, a (200) reflection changes the tilt angle from 106.5° to 104° as represented by the arrows in Figure 8. The shift of tilt angles is accompanied by a discon-

Table 1. Tilted, Hexagonal Columnar Phase in the coTPP-7/11(9/1)

	(hk0)	(hk0) wrt equator (deg)	d spacing (nm)	unit cell parameters $a = 2d_{200}/\sin\beta'$, $b = \sqrt{3}a$	$d_{(200)}/d_{(110)}$ (calculated)	$d_{(200)}/d_{(110)}$ (measured)
(1)	(200)	25	0.423	$a = 0.93$ nm	0.931	0.928
	(110)	~12	0.456	$b = 0.54$ nm, $\beta' = 115°$		
(2)	(200)	22	0.431	$a = 0.93$ nm	0.946	0.944
	(110)	~11.5	0.456	$b = 0.54$ nm, $\beta' = 112°$		
(3)	(200)	19.5	0.438	$a = 0.93$ nm	0.955	0.954
	(110)	~10	0.460	$b = 0.54$ nm, $\beta' = 109.5°$		
(4)	(200)	17	0.445	$a = 0.93$ nm	0.967	0.968
	(110)	~9	0.460	$b = 0.54$ nm, $\beta' = 107°$		
(5)	(200)	4	0.464	$a = 0.93$ nm	0.998	0.997
	(110)	2	0.465	$b = 0.54$ nm, $\beta' = 94°$		

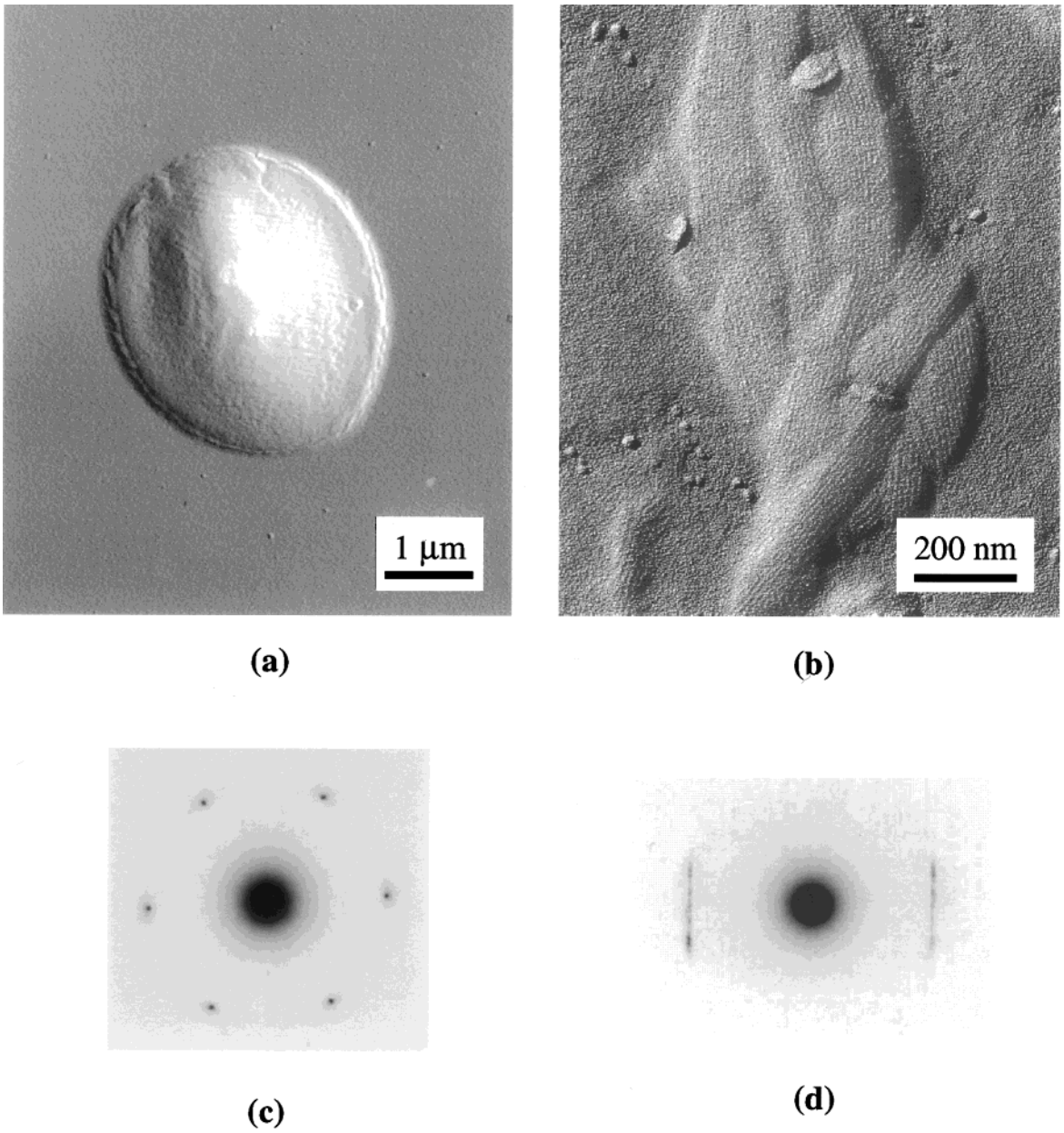

Figure 6. TEM morphological observation and ED results from the coTPP-7/11(5/5): (a) a single domain morphology; (b) a polydomain morphology; (c) an ED pattern obtained from (a): homeotropic chain orientation; (d) an ED pattern obtained from (b): homogeneous chain orientation.

tinuous change in the reflection d spacings. Figure 9 shows the d spacing change of several sets of reflections as a function of temperature. A linear relationship between d spacing and temperature exists below 100 °C and above 130 °C for each reflection. Two d spacings and two tilt angles coexist between 110 and 120 °C as shown in this figure for the (200) reflection with the β' changed from 106.5° to 104°, which is the most evident among all the reflections. Between 100 and 130 °C, a jump in d-spacing can be found for each set of the reflections, corresponding to a thermodynamic first-order transition. The β' tilt angles of 106.5°, 109°, and

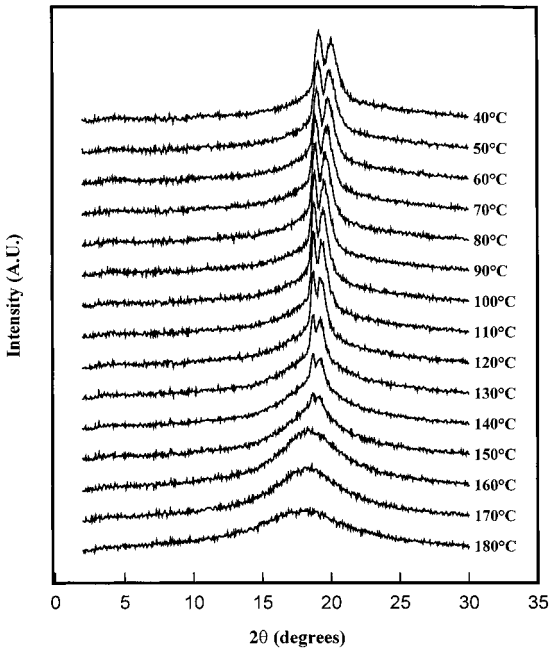

Figure 7. WAXD powder patterns for the coTPP-7/11(7/3) at various temperatures.

111.5° observed below 100 °C shift to 104°, 106°, and 109° after the transition. The low-temperature phase of all the coTPPs-7/11 has been assigned as a Φ_{TH} phase, in which the molecular chains are packed in the same *a* and *b* dimensions in a two-dimensional hexagonal lattice having multiple tilt angles. After this low-temperature transition, the columnar phase (Φ') can be identified due to the highly ordered lateral packing but is no longer hexagonal since the lattice has been distorted by the different thermal expansions of the (200) and (110) planes. Because of the decrease in intensity of the reflections and the more severe overlap caused by the smaller tilt angles above 130 °C, the symmetry of the lateral packing of the Φ' phase is difficult to determine. However, to the best of our knowledge, this is the first time that a columnar−columnar phase transition has been observed in a main-chain LC polymer.

We speculate that the conformational change of the methylene units accounts for this columnar−columnar phase transition and should be detectable by FTIR experiments. Generally, in the amorphous phase of polymer systems, the existence of various kinds of conformations has to be considered.[33] Figure 10 is a plot of the temperature dependence of the IR spectrum of the coTPP-7/11(7/3) in the CH_2 bending region. The shoulder near 1468 cm^{-1} increases in intensity with respect to the intensity of 1475 cm^{-1} band when the temperature increases. The 1475 cm^{-1} band can be assigned as $-gt_mg'-$ type with a *trans*-dominated (*m*, large) conformation, whereas the 1468 cm^{-1} band is associated with a *gauch*-dominated (*m*, small) conformation.[34] The IR observation in the coTPP-7/11(7/3) reveals that the *trans*-conformation content of the (CH_2) segments is gradually reduced upon heating. Let N_1 and N_2 be the population of two conformers with *trans*- and *gauch*-conformation, respectively, this may give rise to two IR bands with intensities $I_1 = \alpha_1 N_1$ and $I_2 = \alpha_2 N_2$ where α_1 and α_2 are the absorption coefficients of the corresponding modes. The spectral deconvolution was used to evaluate the two conformers, and the relative population of N_1/N_2 is given by the Boltzman relation. The temperature-dependent relative population of the two conformers, $\ln(I_1/I_2)$, is plotted as a function of $1/T$ in Figure 11. The slope changes at approximately 110 °C and is consistent with the WAXD fiber experiments. This should correspond to the low-temperature transition, which results from the cumulative change in the population of the *trans*- and *gauch*-conformation, and thus is associated with conformational disorder.[35] Similar observations can also be found for all coTPPs-7/11 with other comonomer compositions.

After the columnar−columnar phase transition, the WAXD reflection intensities decrease further upon heating (see Figure 7). At approximately 160 °C, the Bragg reflections disappear, and only a scattering halo remain. The earlier discussion on DSC results suggests that two transitions remain, which are nearly superimposed within the narrow temperature region. For instance, coTPP-7/11(7/3) is the sample that most clearly presents the two high-temperature transitions among the coTPPs-7/11. The two transitions only have a 1.3

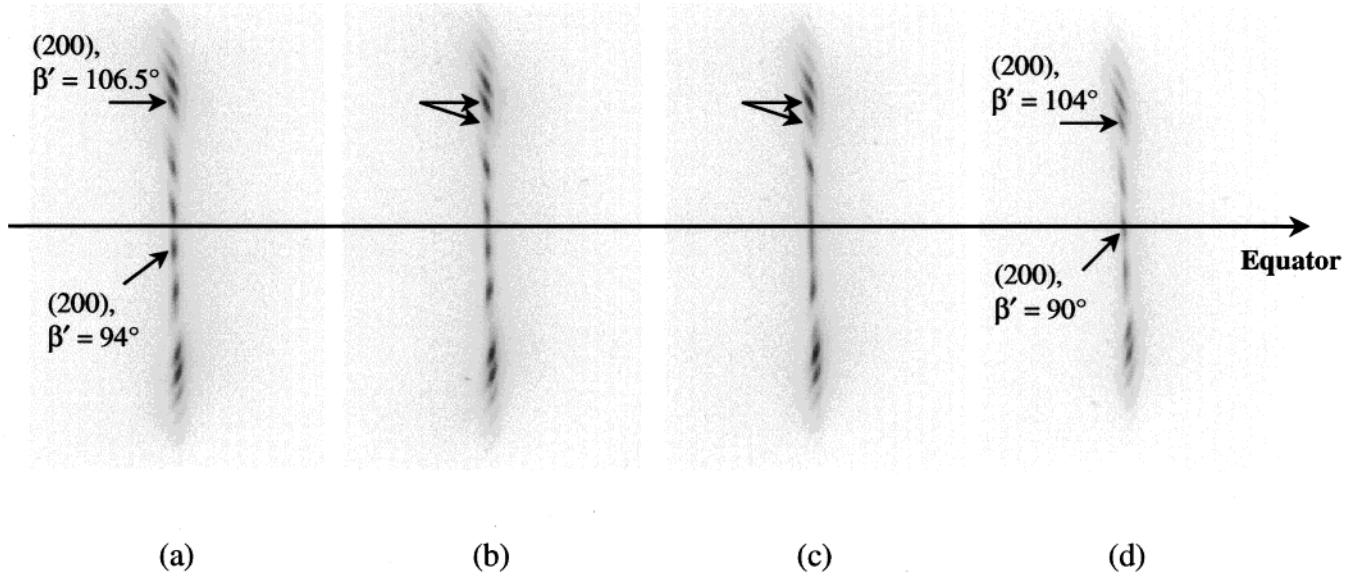

Figure 8. Structure change of the coTPP-7/11(7/3) as shown in the enlarged WAXD fiber patterns during heating: (a) 100, (b) 110, (c) 120, and (d) 130 °C. The horizontal line represents the equatorial direction. The arrows denote the change in patterns.

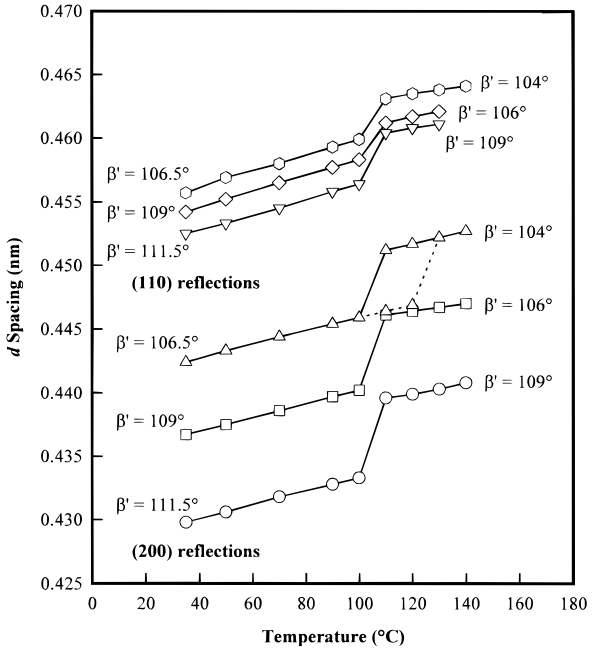

Figure 9. Change in several *d* spacings with respect to temperature for the coTPP-7/11(7/3). Dashed line represents the coexistence of two *d* spacings at 110 and 120 °C.

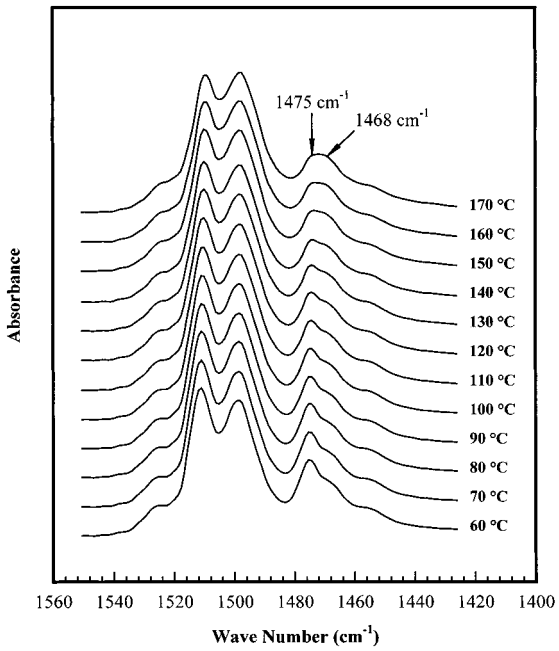

Figure 10. Temperature dependence of the infrared spectra of the coTPP-7/11(7/3) in the CH_2 bending region.

°C difference in peak temperature at a cooling rate of 10 °C/min as shown in Figure 2. A precise structural separation of these two phase transitions in the WAXD patterns is difficult under the temperature resolution of the experiment.

However, PLM observation shows a typical low ordered LC morphology for the sheared samples of all the copolymers. As shown in Figure 12 for the coTPP-7/11(7/3), the banded textures can be clearly seen to be perpendicular to the shear direction following a slight relaxation of the molecules after shearing. Note that the banded textures under an external force field can only be obtained when a sample is in a smectic A, C, or N phase. Since the WAXD patterns do not exhibit any layer reflections for the copolymers in the corresponding

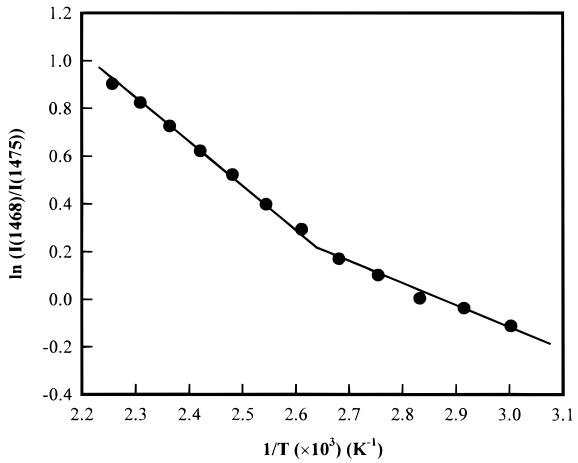

Figure 11. Plot of the relative population of the coTPP-7/11(7/3) as a function of $1/T$ of the infrared bands at 1468 and 1475 cm^{-1}.

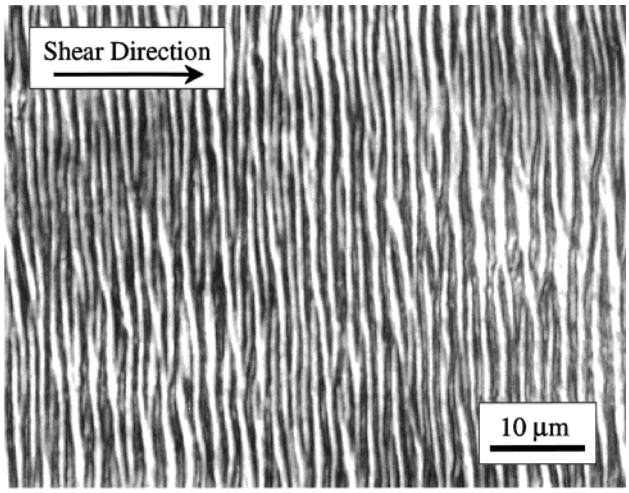

Figure 12. PLM morphological observation of the coTPP-7/11(7/3) after mechanical shearing. The arrow represents the shear direction.

region, a N phase can be determined. In summary, the transition sequence of the coTPP-7/11(7/3) is

$$\text{glassy state} \leftrightarrow \Phi_{TH} \leftrightarrow \Phi' \leftrightarrow \text{N} \leftrightarrow \text{I}$$

As indicated earlier, all the coTPPs-7/11 with the various compositions exhibit the same transition behavior and therefore possess the same transition sequence.

Phase Diagram and Thermal Properties. The phase diagram of the coTPP-7/11 series can be constructed by plotting the equilibrium transition temperatures as a function of composition and is shown in Figure 13. In contrast to the homoTPPs($n = 7$ and 11), the tilted columnar phases are dominant below the N transition temperatures for all of the copolymers. No smectic and smectic crystalline phases are observed, revealing the effect of the mismatch of comonomer lengths on phase structure. Despite its smaller dissimilarity of the two comonomer lengths, the suppression of the layered structure in the coTPPs-7/11 is more severe as compared to the coTPPs-7/12, since both the S_F and SC_G phases can be found in coTPPs-7/12(1/9 and 2/8).[22] On the other hand, the composition change in the coTPPs-7/11 does not play a critical role in the structural order and transition behavior as in the case of the

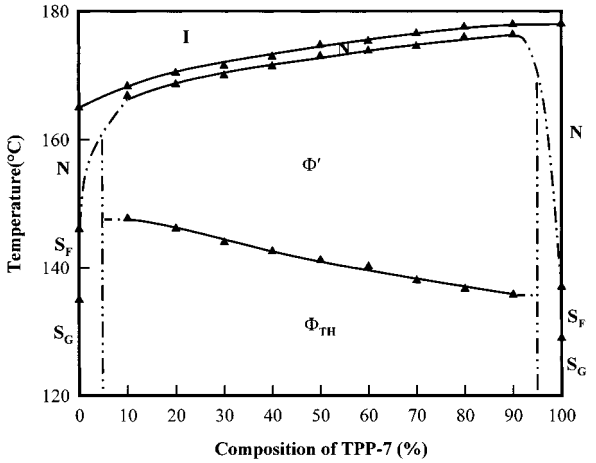

Figure 13. Phase diagram of the coTPPs-7/11 series.

coTPPs-7/12, where the highly ordered smectic and columnar phases are found to be composition-dependent. These comparisons indicate the different molecular packing schemes between the odd−odd and odd−even systems of coTPPs.

The enthalpy of these phase transitions is composition-dependent. For the columnar−columnar phase transition, the enthalpy decreases almost linearly with increasing composition of TPP($n = 7$) from 7.5 kJ/mol for coTPP-7/11(1/9) to 5.7 kJ/mol for coTPP-7/11(9/1). This accounts for an approximate 0.2 kJ/mol decrease for the incorporation of every 10% of TPP($n = 7$). The transition entropy can be calculated based on the equation of $\Delta S = \Delta H/T$, yielding 17.8 J/(K mol) for coTPP-7/11(1/9) and 13.9 J/(K mol) for coTPP-7/11(9/1). This is also close to a linear relationship with respect to the composition. Since the high-temperature transitions, which correspond to the $\Phi' \rightarrow$ N and N $\rightarrow$ I phase transitions, are overlapped within a narrow temperature region, their enthalpies are more difficult to obtain. However, the combined enthalpy change for the $\Phi' \rightarrow$ I transitions decreases linearly from 9.1 kJ/mol in coTPP-7/11(1/9) to 6.7 kJ/mol in coTPP-7/11(9/1), approximately 0.5 kJ/mol larger than the value for the N $\rightarrow$ I transition assuming the linear addition from homoTPPs($n = 7$ and 11). The peak separation results from several samples such as coTPPs-7/11(1/9 and 5/5) indicate that the enthalpy ratio of the two transitions is approximately 1:1. Although these transitions possess 100% phase changes from one phase to another, this ratio indicates that in coTPPs-7/11, the N $\rightarrow$ I transition enthalpy is much smaller than that predicted by the linear relationship between TPPs($n = 7$ and 11). This may result from a less perfect order in the N phase, disturbed by the inclusion of comonomers in the chain packing. Furthermore, these small transition enthalpies also indicate that these mesophases possess high molecular mobility, which has also been identified by our preliminary results on solid-state ^{13}C nuclear magnetic resonance experiments.[7] The research along this line is currently undertaken.

The glass transition temperatures (T_g) of all of the coTPP-7/11 are approximately between 26 and 37 °C. A tendency can be recognized that with increasing the composition of TPP($n = 7$) comonomer the T_g is slightly increased. Figure 14 shows DSC heating curves of coTPP-7/11 in the T_g region. Note that the T_g's of homoTPP($n = 7$ and 11) are 26 and 37 °C, respectively. However, both the homopolymers at room temperature

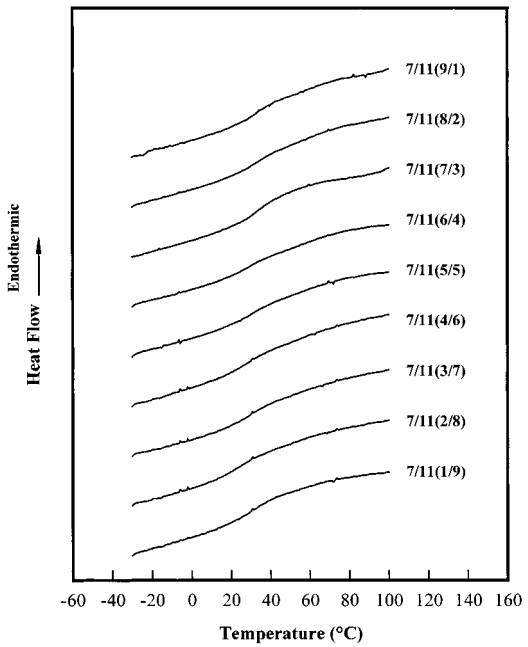

Figure 14. Set of DSC heating curves for the coTPPs-7/11 in their T_g regions.

are in highly ordered smectic phases, while coTPPs-7/11 are in the Φ_{TH} phase. It is interesting to find that the heat capacity increases at T_g for all these coTPPs-7/11 are only in a range of 60−80 J/(K mol), which is only approximately one-third of the estimated heat capacity increase for amorphous coTPPs-7/11 based on the group addition scheme.[36] This indicates that the two-dimensional ordered Φ_{TH} phase does limit molecular motion above the T_g.

Conclusion

For the series of coTPPs-7/11 with comonomer compositions from 1/9 to 9/1, the phase structure and transition behavior are identical. The low-temperature phase for these copolymers is a Φ_{TH} phase possessing multiple tilt angles between the molecular axes and the hexagonal normal. However, the same two-dimensional lateral lattice (*a* and *b* dimensions) are observed disregarding the difference in tilt angles. No long-range order can be found along the column direction. Upon heating, the Φ_{TH} phase transforms to a Φ' phase based on the changes in fiber patterns of the temperature-resolved WAXD experiments. All of the reflections representing the lateral orders shift toward the equator during the transition accompanied by the decreased tilt angles. This columnar−columnar phase transition is thermodynamically first-order, which is attributed to the conformational change in the methylene units as evidenced using FTIR analyses. Further increase in temperature leads to the two overlapped transitions to the N phase and the isotropic melt. These transitions exhibit small transition enthalpies, indicating that these columnar phases possess relatively poor structural order. The T_g's of coTPPs-7/11 are found to be slightly comonomer composition dependent, and molecular motion above the T_g is limited by the columnar phase.

Acknowledgment. This work was supported by the National Science Foundation (DMR-96-17030) and the Science and Technology Center for Advanced Liquid Crystal Optical Materials (ALCOM) at Kent State

University, Case Western Reserve University, and the University of Akron. Support from the Chinese National Natural Science Foundation for promoting scientific collaborations is also acknowledged.

References and Notes

(1) Cheng, S. Z. D.; Yoon, Y.; Zhang, A.; Savitski, E. P.; Park, J.-Y.; Percec, V.; Chu, P. *Macromol. Rapid Commun.* **1995**, *16*, 533.
(2) Yoon, Y.; Zhang, A.; Ho, R.-M.; Cheng, S. Z. D.; Percec, V.; Chu, P. *Macromolecules* **1996**, *29*, 294.
(3) Yoon, Y.; Ho, R.-M.; Moon, B.; Kim, D.; McCreight, K. W.; Li, F.; Harris, F. W.; Cheng, S. Z. D.; Percec, V.; Chu, P. *Macromolecules* **1996**, *29*, 3421.
(4) Yoon, Y.; Ho, R.-M.; Savitski, E. P.; Li, F.; Cheng, S. Z. D.; Percec, V.; Chu, P. In *Liquid-Crystalline Polymer Systems Technological Advances*; ACS Symposium Series 632; American Chemical Society: Washington, DC, 1996; pp 358−371.
(5) Yoon, Y.; Ho, R.-M.; Li, F.; Moon, B.-S.; Park, J.-Y.; Harris, F. W.; Cheng, S. Z. D.; Percec, V.; Chu, P. *J. Therm. Anal.* **1996**, *47*, 957.
(6) Yoon, Y.; Ho, R.-M.; Li, F.; Leland, M.; Park, J.-Y.; Cheng, S. Z. D.; Percec, V.; Chu, P. *Prog. Polym. Sci.* **1997**, *22*, 765.
(7) Cheng, J.; Yoon, Y.; Ho, R.-M.; Leland, M.; Guo, M.; Cheng, S. Z. D.; Percec, V.; Chu, P. *Macromolecules* **1997**, *30*, 4688.
(8) Ho, R.-M.; Yoon, Y.; Leland, M.; Cheng, S. Z. D.; Yang, D.; Percec, V.; Chu, P. *Macromolecules* **1996**, *29*, 4528.
(9) Ho, R.-M.; Yoon, Y.; Lelend, M.; Cheng, S. Z. D.; Percec, V.; Chu, P. *Macromolecules* **1997**, *30*, 3349.
(10) Shadashiva, B. K.; Suresh, K. A. *Pramana* **1977**, *9*, 471.
(11) Destrade, C.; Malthete, J.; Tinh, N. H.; Gasparoux, H. *J. Phys., Lett.* **1980**, *78A*, 82.
(12) Destrade, C.; Tinh, N. H.; Gasparoux, H.; Malthete, J.; Levelut, A. M. *Mol. Cryst. Liq. Cryst.* **1981**, *71*, 111.
(13) Levelut, A. M.; Malthete, J. *Mol. Cryst. Liq. Cryst.* **1984**, *106*, 121.
(14) Malthete, J.; Levelut, A. M.; Tinh, N. H. *J. Phys., Lett.* **1985**, *46*, 875.
(15) Destrade, C.; Tinh, N. H.; Roubineau, A.; Levelut, A. M. *Mol. Cryst. Liq. Cryst.* **1988**, *159*, 163.
(16) Chandrasekhar, S.; Ranganath, G. S. *Rep. Prog. Phys.* **1990**, *53*, 57.
(17) Kreuder, W.; Ringsdorf, H.; Tschirner, P. *Makromol. Chem., Rapid Commun.* **1985**, *6*, 367.
(18) Ringsdorf, H.; Tschirner, P.; Herrmann-Schonheer, O.; Wendorff, T. H. *Makromol. Chem.* **1987**, *188*, 1431.
(19) Ungar, G. *Polymer* **1993**, *34*, 2050.
(20) Unger, G.; Feijoo, J. L.; Percec, V.; Yourd, R. *Macromolecules* **1991**, *24*, 953.
(21) Zheng, R.-Q.; Chen, E.-Q.; Cheng, S. Z. D.; Xie, F.; Yan, D.; He, T.; Percec, V.; Chu, P.; Ungar, G. *Macromolecules* **1999**, *32*, 3574.
(22) Zheng, R.-Q.; Chen, E.-Q.; Cheng, S. Z. D.; Xie, F.; Yan, D.; He, T.; Percec, V.; Chu, P.; Ungar, G. *Macromolecules* **1999**, *32*, 6981.
(23) Percec, V.; Chu, P.; Ungar, G.; Cheng, S. Z. D.; Yoon, Y. *J. Mater. Chem.* **1994**, *4*, 719.
(24) Yandrasits, A.; Cheng, S. Z. D.; Zhang, A.; Cheng. J.; Wunderlich, B.; Percec, V. *Macromolecules* **1992**, *25*, 2112.
(25) Pardey, R.; Harris, F. W.; Cheng, S. Z. D.; Adduci, J.; Facinelli, J. V.; Lenz, R. W. *Macromolecules* **1992**, *25*, 5060.
(26) Pardey, R.; Shen, D.; Gabori, P. A.; Harris, F. W.; Cheng, S. Z. D.; Adduci, J.; Facinelli, J. V.; Lenz, R. W. *Macromolecules* **1993**, *26*, 3687.
(27) Ge, J. J.; Zhang, A.; McCreight, K. W.; Ho, R.-M.; Wang, S.-Y.; Jin, X.; Harris, F. W.; Cheng, S. Z. D. *Macromolecules* **1997**, *30*, 6498.
(28) Ge, J. J.; Honigfort, P. S.; Ho, R.-M.; Wang, S.-Y.; Jin, X.; Harris, F. W.; Cheng, S. Z. D. *Macromol. Chem. Phys.* **1999**, *200*, 31.
(29) Gray, G. W.; Goodby, J. W. G. *Smectic Liquid Crystals: Textures and Structures*; Leonard Hill: London, 1984.
(30) Pershan, P. S. *Structure of Liquid Crystal Phases*; World Scientific: Singapore, 1988.
(31) De Genes, P. G.; Prost, J. *The Physics of Liquid Crystals*; Oxford: New York, 1993.
(32) Chaikin, P. M.; Lubensky, T. C. *Principle of Condensed Matter Physics*; Cambridge: New York, 1995.
(33) Radice, S.; Fanti, N. D.; Zerbi, G. *Polymer* **1997**, *38*, 2753.
(34) Painter, P. C.; Coleman, M. M.; Koenig, J. L. *The Theory of Vibrational Spectroscopy and its Application to Polymer Materials*; John Wiley & Sons: New York, 1982; Chapter 15.
(35) Wunderlich, B.; Moller, M.; Grebowicz, J.; Baur, H. *Adv. Polym. Sci.* **1988**, *87*, 1.
(36) Wunderlich, B. *Thermal Analysis*; Academic Press: San Diego, 1990; Chapter 5.

MA991963P